involved are summarized in Table III. In $Hg_4(AsF_6)_2$, however, the interaction of the Hg_4^{2+} ion with the AsF_6^- anion in a direction approximately collinear with the terminal Hg–Hg bonds is replaced by the intercation Hg···Hg interaction at 124° to the terminal Hg–Hg bond and several weak Hg···F contacts with the anions. These latter Hg···F interactions are considerably longer than the short interactions (2.38 Å) in $Hg_3(AsF_6)_2$,[2] which are collinear with the Hg–Hg bonds. They resemble in length the interactions in other compounds that are not collinear with the Hg–Hg bonds. For example, the closest Hg···F contacts in $Hg_{2.86}AsF_6$ are 2.87 (1) or 2.98 (1) Å.[1,15]

If the intercation Hg···Hg contact and one or two of the shortest Hg···F contacts to Hg(1) are considered, then the environment of Hg(1) in $Hg_4(AsF_6)_2$ is similar to that of the Hg atoms in the two modifications of tetrakis(diphenylseleno)dimercury(I) perchlorate, $[(C_6H_5)_2Se]_4Hg_2(ClO_4)_2$.[16] Other interionic interactions of comparable strength in other Hg(I) and Hg(II) compounds have been observed, and many of these are discussed elsewhere.[17] However, the nature of these additional interactions is still unclear. A recent calculation[18] on the mercurous halides Hg_2F_2 and Hg_2Cl_2 indicated that the closest next-neighbor fluorine and chlorine atoms might be close enough to transfer charge into the LUMO of the Hg_2Cl_2 (or Hg_2F_2) molecule, strengthening the Hg–Hg bond and weakening the Hg–Cl bond. However, in $Hg_3(AlCl_4)_2$ there is no correlation between the Hg–Hg bond lengths and the adjacent collinear Hg···Cl interactions, since the long Hg–Hg bond (2.562 Å) is collinear with the long Hg···Cl interaction (2.562 Å) and the short Hg–Hg bond (2.551 Å) is collinear with a short Hg···Cl interaction (2.517 Å) (Table III). However evidence of the charge-transfer interaction in this case can certainly be seen in terms of a lengthening of the two Al–Cl bonds involved.[14] The lengths of the remaining longer intermolecular Hg···Cl contacts in this and other structures may then be of importance in explaining these observed bond length trends. The standard deviations on the distances generally precludes a similar observation in the present compound although we may note that the longer As–F bonds (1.75 (4) and 1.71 (3) Å) are to the fluorine atoms involved in the shortest Hg···F contacts. The crystal packing indicated in Figure 2 consists of layers of mercury chains interspersed with layers of hexafluoroarsenate anions along *a*.

Acknowledgment. We thank the Natural Sciences and Engineering Research Council of Canada for financial support of this work.

Registry No. $Hg_4(AsF_6)_2$, 51383-33-6; AsF_5, 7784-36-3; Hg, 7439-97-6.

Supplementary Material Available: A listing of structure factor amplitudes for $Hg_4(AsF_6)_2$ (7 pages). Ordering information is given on any current masthead page.

(15) Schultz, A. J.; Williams, J. M.; Miro, N. D.; MacDiarmid, A. G.; Heeger, A. S. *Inorg. Chem.* **1978**, *17*, 646.
(16) Brodersen, K.; Liehr, G.; Rosenthal, M.; Thiele, G. *Z. Naturforsch., B: Anorg. Chem., Org. Chem.* **1978**, *33B*, 1227.
(17) Kuz'mina, L. G.; Bokii, N. G.; Struchtov, Yu. T. *Russ. Chem. Rev. (Engl. Transl.)* **1975**, *44*, 73.
(18) Kleier, D. A.; Wadt, W. R. *J. Am. Chem. Soc.* **1980**, *102*, 6909.

Contribution from the Arthur Amos Noyes Laboratory, Division of Chemistry and Chemical Engineering, California Institute of Technology, Pasadena, California 91125

Electrochemistry of the Trinuclear Aquo Mo^{IV}_3 and Mo^{III}_3 Ions in Acidic Media

MARK T. PAFFETT and FRED C. ANSON*

Received August 25, 1982

The trinuclear ions containing Mo(IV), $Mo_3O_4(H_2O)_9^{4+}$ (Mo^{IV}_3) and the oxalato derivative $Mo_3O_4(C_2O_4)_3(H_2O)_3^{2-}$, can be reversibly reduced in acidic media to trinuclear Mo(III) species. The reductions involve two sequential electron-transfer steps with formal potentials that are pH dependent:

$$Mo^{IV}_3 + 2e^- \overset{E^f_1}{\rightleftharpoons} Mo^{III}_2Mo^{IV} \qquad Mo^{III}_2Mo^{IV} + 1e^- \overset{E^f_2}{\rightleftharpoons} Mo^{III}_3$$

Two waves are evident in voltammograms and polarograms of $Mo_3O_4(C_2O_4)_3(H_2O)_3^{2-}$, but with Mo^{IV}_3 the two formal potentials are too close together to observe separate waves. However, logarithmic analysis of the shapes of normal-pulse polarograms allowed the two formal potentials to be evaluated. The reductions of both complexes are believed to be accompanied by protonation of the bridging and capping oxo ligands. The new, trinuclear Mo^{III}_3 species resulting from the three-electron reduction of Mo^{IV}_3 exhibits a characteristic ESR spectrum. The mixed-valent intermediate, $Mo^{III}_2Mo^{IV}$, is diamagnetic. Possible structural changes that accompany the addition of electrons and protons to Mo^{IV}_3 are discussed.

The crystal structures of ions containing molybdenum in oxidation state IV have been determined for anionic complexes containing oxalate[1] and edta[2] (edta = ethylenediaminetetraacetate) as ligands. In both of these cases the structures are based upon a trimeric core of composition $Mo_3O_4^{4+}$ (Figure 1). In addition, the structure of an isothiocyanato complex has been surmised.[3] Earlier studies[4] had suggested a dimeric structure for the aquo Mo(IV) ion, which was the assumption made in a previous report from this laboratory.[6] Since more recent structural studies seem to show conclusively that aquo Mo(IV) is trimeric,[3,7] we have reexamined the electrochemistry of this ion in greater detail to see whether it is consistent with the presence of three reducible centers in the ion. While this study was in progress, Richens and Sykes reported the results of experiments on aquo Mo(IV) that included some electrochemical measurements.[8,9] Where they overlapped, our ex-

(1) Bino, A.; Cotton, F.; Dori, Z. *J. Am. Chem. Soc.* **1978**, *100*, 5252.
(2) Bino, A.; Cotton, F.; Dori, Z. *J. Am. Chem. Soc.* **1979**, *101*, 3842.
(3) Murmann, R.; Shelton, M. *J. Am. Chem. Soc.* **1980**, *102*, 3984.
(4) Ardon, M.; Pernick, A. *J. Less-Common Met.* **1977**, *54*, 233.
(5) Ardon, M.; Pernick, A. *J. Am. Chem. Soc.* **1973**, *95*, 6871.
(6) Chalilpoyil, P.; Anson, F. *Inorg. Chem.* **1978**, *17*, 2418.
(7) Cramer, S.; Eidem, P.; Paffett, M.; Winkler, J.; Dori, Z.; Gray, H. *J. Am. Chem. Soc.* **1983**, *105*, 799–802.
(8) Richens, D.; Sykes, A. *Inorg. Chim. Acta* **1981**, *54*, L3–L4.
(9) Richens, D.; Sykes, A. *Inorg. Chem.* **1982**, *21*, 418.

0020-1669/83/1322-1347$01.50/0

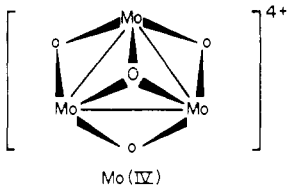

Figure 1. Core structure of trimeric Mo^{IV}_3 complexes.[1,2]

perimental observations coincided with those described by Richens and Sykes[9] although we will offer different interpretations of some of the electrochemical responses exhibited by the aquo Mo^{IV}_3 ion.

Experimental Section

Materials. $Cs_2Mo_3O_4(C_2O_4)_3(H_2O)_3$ was synthesized according to a published procedure.[1] Mo^{IV}_3 aquo ion was prepared as previously described[6] and further purified by ion exchange on a (Bio-Rad) AG50W-2X cation-exchange column (14 × 2 cm). The concentration of Mo^{IV}_3 was determined by titration with a standard solution of Ce(IV). The molar absorbance of Mo^{IV}_3 at 508 nm in 2 M trifluoromethanesulfonic acid was measured as $\epsilon_{508} = 192\ M^{-1}\ cm^{-1}$, which agreed with a previously reported value[10] in *p*-toluenesulfonic acid. Solutions of what is almost certainly Mo^{III}_3 were prepared by controlled-potential reduction of Mo^{IV}_3 at a mercury-pool electrode.

Trifluoromethanesulfonic acid (Minnesota Mining and Manufacturing Co.) was purified by distillation as described previously.[6] The concentrated, purified acid was diluted with distilled water that had been further purified by passage through a purification train (Barnstead Nanopure D2790). Stock solutions of lithium trifluoromethanesulfonate were prepared by neutralization of reagent grade Li_2CO_3. Other reagent grade materials were used as received. *o*-Nitroaniline (Aldrich Chemical Co.) was recrystallized twice. Solutions were deoxygenated by bubbling with prepurified argon.

Instrumentation and Techniques. Spectra were recorded on a Cary 17 or a Hewlett-Packard 8450A spectrophotometer. ESR spectra were recorded on a Varian E-Line Century Series spectrometer. Cyclic voltammetry and pulse polarography were conducted with a PAR (EG&G Instrument Co., Princeton, NJ) Model 174 instrument that had been modified to provide variable pulse width.[11] Controlled-potential electrolyses were carried out with a PAR Model 173 potentiostat and Model 179 digital coulometer. To permit spectra of air-sensitive electrolysis solutions to be recorded without removal from the electrolysis cell, an H-cell with a spectroscopic cuvette attached by an L-shaped arm was constructed. During electrolysis the solution level was below the inlet to the cuvette. To record spectra, the cell was tipped to fill the cuvette and the process was reversed when additional electrolysis was desired. Potentials were measured and are reported with respect to a saturated calomel electrode. A dropping-mercury electrode with a mercury flow rate of 0.7–1.2 mg s^{-1} was employed to record polarograms. Cyclic voltammograms were obtained with a hanging mercury drop electrode having an area of 0.032 cm^2. Potentials were measured and are reported with respect to a saturated calomel electrode (SCE).

Results

The Tris(oxalato) Complex of Mo(IV). The complete formula of the tris(oxalato) complex is $Mo_3O_4(C_2O_4)_3(H_2O)_3^{2-}$.[1] Hereafter, we will omit the water molecules in writing the formula of this complex. An earlier polarographic study[12] of the $Mo_3O_4(C_2O_4)^{2-}$ ion reported the presence of two reduction waves, but possible structural changes accompanying its reduction were not considered. Cyclic voltammograms of $Mo_3O_4(C_2O_4)_3^{2-}$ exhibit two well-separated reduction steps (Figure 2). The separation of the two steps simplifies the interpretation of the behavior of this complex. For this reason, we will consider it first because the behavioral pattern it exhibits will prove useful in understanding that of the Mo^{IV}_3 aquo ion to be described subsequently.

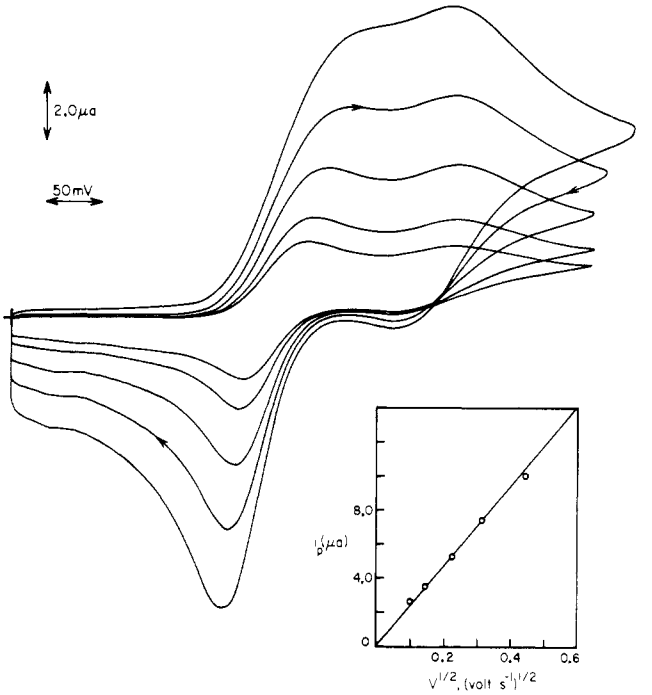

Figure 2. Cyclic voltammograms of 0.8 mM $Mo_3O_4(C_2O_4)_3^{2-}$ in 0.1 M ($H_2C_2O_4 + K_2C_2O_4$) at pH 1.53. The ionic strength was adjusted to 0.5 M with KCl (initial potential −300 mV; scan rates 10, 20, 50, 100, and 200 mV s^{-1}). Negative potentials are plotted to the right and reduction currents are plotted upward. Inset: Peak current vs. (scan rate)$^{1/2}$ for the first cathodic peak.

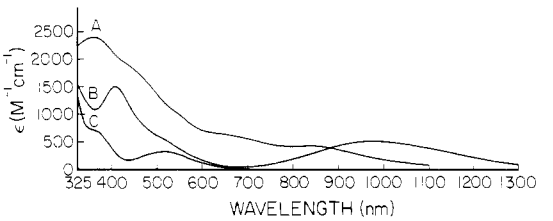

Figure 3. Spectra of (A) $Mo_3(OH)_4(C_2O_4)_3^-$, (B) $Mo_3(OH)_4(C_2O_4)_3$, and (C) $Mo_3O_4(C_2O_4)_3^{2-}$ in 0.5 M $H_2C_2O_4$.

The magnitudes of the cathodic peak currents in Figure 2 are consistent with a two-electron step followed by a one-electron step. The first reduction peak is diffusion controlled, as determined from the plot of its peak current vs. (scan rate)$^{1/2}$ (Figure 2). The separation between the cathodic and anodic peak potentials of the first wave increases as the scan rate increases, as expected if the electrode reaction were only quasi-Nernstian. At a scan rate of 10 mV s^{-1} the peaks are separated by 55 mV compared with the 30-mV separation expected for a two-electron Nernstian reaction (or the 60 mV expected if the reduction involved only one electron). The second reduction process is also diffusion controlled with an invariant peak splitting of 60 mV. Electrolyte composition had no effect on the peak splitting of the second wave; however, adsorption of the reactant was evident in solutions free of chloride ion. The chloride was added to the supporting electrolyte employed to record Figure 2 both to adjust the ionic strength and to suppress this adsorption.

Controlled-potential reduction of $Mo_3O_4(C_2O_4)_3^{2-}$ in 0.5 M oxalic acid consumes 2 faradays/mol of complex when the electrode is held at a potential slightly negative of the first wave (−600 mV). At more negative potentials (e.g., −900 mV) 3 faradays/mol of complex is consumed. The fully reduced species is stable in the absence of air for at least 1 week. Its spectrum is shown in Figure 3 (curve A) along with that of

(10) Ojo, J.; Sosaki, Y.; Taylor, R.; Sykes, A. *Inorg. Chem.* **1976**, *15*, 1006.
(11) Abel, R.; Christie, J.; Jackson, L.; Osteryoung, J.; Osteryoung, R. *Chem. Instrum. (N.Y.)* **1976**, 123.
(12) Wendling, E.; Rohmer, R. *Bull. Soc. Chim. Fr.* **1964**, 360.

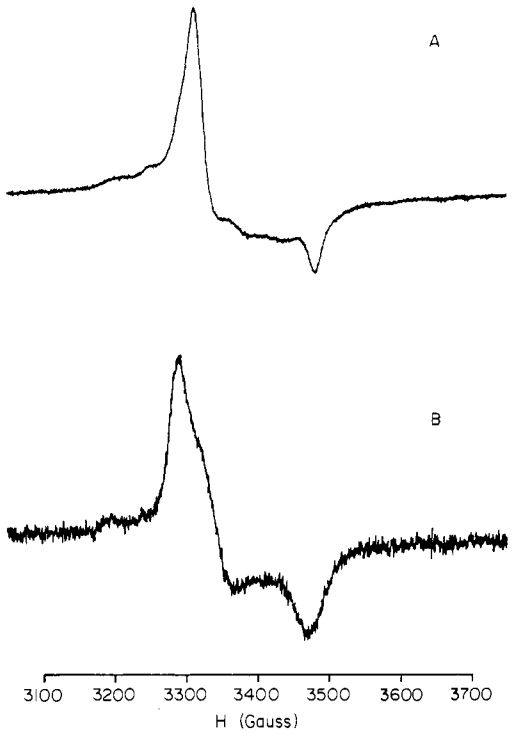

Figure 4. ESR spectra of (A) $Mo_3(OH)_4(C_2O_4)_3^-$ and (B) aquo Mo^{III}_3 ion. Microwave frequencies and modulation amplitudes: (A) 9.225 GHz, 1 G; (B) 9.168 GHz, 2 G.

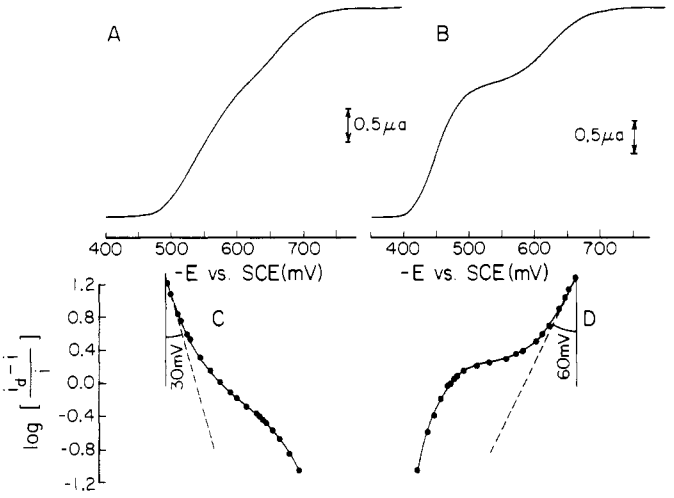

Figure 5. Normal- (A) and reverse-pulse (B) polarograms of 0.8 mM $Mo_3O_4(C_2O_4)_3^{2-}$ (supporting electrolyte as in Figure 2). Parts C and D are the corresponding plots of log $[(i_d - i)/i]$ vs. E (see text).

the original complex (curve C). A spectrum of the two-electron-reduction product is also shown in Figure 3 (curve B), but the solution also contains a small amount (~5%) of the fully reduced complex whose formation is difficult to avoid at the potential where the two-electron product is generated at a convenient rate.

The fully reduced ion exhibited the ESR spectrum shown in Figure 4A in a frozen solution at 77 K. Solutions of the two-electron-reduction product showed only a very weak ESR response under the same conditions.

Pulse Polarography. Normal- and reverse-pulse polarograms[13] for solutions of $Mo_3O_4(C_2O_4)_3^{2-}$ also contain two reduction steps (Figure 5). The separation between the two steps is larger in the reverse-pulse polarograms (Figure 5B)

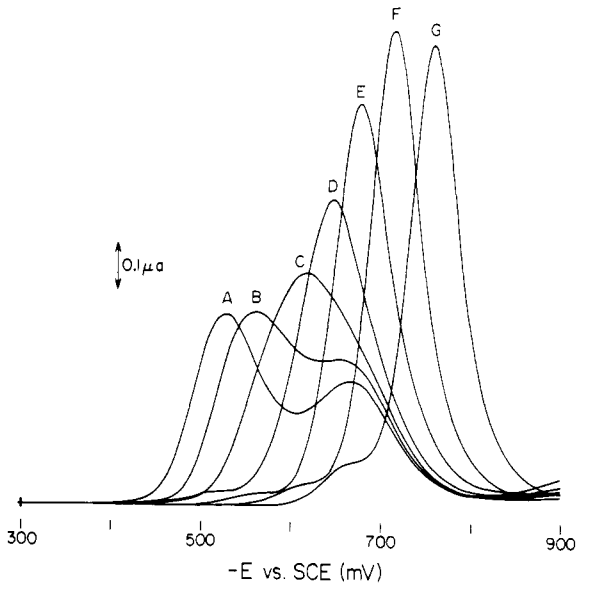

Figure 6. Differential-pulse polarograms of $Mo_3O_4(C_2O_4)_3^{2-}$ as a function of pH. All solutions contained 0.1 M total oxalate, and the ionic strength was maintained at 0.5 M with KCl. The pH values were (A) 1.25, (B) 1.57, (C) 1.95, (D) 2.49, (E) 3.05, (F) 3.85, and (G) 4.69.

because of the differing electron-transfer kinetics exhibited by the two reduction steps: the half-wave potential of the two-electron, quasi-Nernstian step is shifted to a more positive value in the reverse-pulse polarogram while that of the one-electron Nernstian step remains fixed. The two well-developed limiting currents in the reverse-pulse polarogram have the expected ratio of 2:1. The shapes of the normal- and reverse-pulse polarographic waves were analyzed by plotting log $[(i_d - i)/i]$ as a function of the electrode potential.[15,16] The results are shown in curves C and D of Figure 5. The slope of the logarithmic plot corresponding to the foot of the first reduction wave is close to 30 mV/decade, as expected for a two-electron reaction. The slope increases as the wave is ascended, and the quasi-Nernstian character of the wave is expressed. The corresponding plot for the first oxidation wave in the reverse-pulse polarogram has a slope near 60 mV over most of the wave, as expected for a Nernstian one-electron reaction.

The two reduction steps evident in Figure 5A are more clearly separated when their derivatives are recorded as in differential-pulse polarography.[14] Figure 6 shows a set of differential-pulse polarograms for a series of $Mo_3O_4(C_2O_4)_3^{2-}$ solutions with varying pH. The peak corresponding to the first, two-electron, reduction shifts to more negative values as the pH increases until it merges with the second, one-electron, peak whose position is insensitive to pH before the merger. The single peak remaining after the reduction steps have coalesced continues to shift to more negative potentials with further increases in pH. (The small wave appearing at the foot of the main waves in Figure 6 arose from slight air oxidation of the $Mo_3O_4(C_2O_4)_3^{2-}$ stock solution. The wave is not present in freshly prepared solutions.) The peak potentials of the first (or merged) wave in Figure 6 are plotted vs. pH in Figure 7. At pH values of 2 and below the first wave shifts by 120 mV/pH unit while the peak potential of the coalesced wave shifts by 52 mV/pH unit.

(13) Bard, A. J.; Faulkner, L. "Electrochemical Methods"; Wiley: New York, 1981, p 186.
(14) Reference 13, p 190.
(15) Oldham, K.; Parry, E. *Anal. Chem.* **1968**, *40*, 65.
(16) Matsuda, H. *Bull. Chem. Soc. Jpn.* **1980**, *53*, 3439.

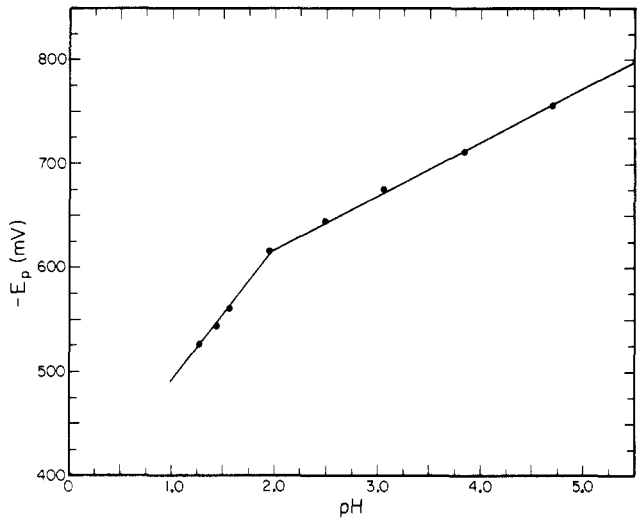

Figure 7. Differential-pulse polarographic peak potentials vs. pH for the reduction of $Mo_3O_4(C_2O_4)_3^{2-}$ (conditions as in Figure 6).

These electrochemical results can be accommodated by the series of electrode reactions depicted in Scheme I.

Scheme I

pH <2

first step: $Mo_3O_4(C_2O_4)_3^{2-} \underset{-2e^-,\,-4H^+}{\overset{+2e^-,\,+4H^+}{\rightleftharpoons}} Mo_3(OH)_4(C_2O_4)_3$

quasi-Nernstian

second step: $Mo_3(OH)_4(C_2O_4)_3 \underset{-e^-}{\overset{+e^-}{\rightleftharpoons}} Mo_3(OH)_4(C_2O_4)_3^-$

Nernstian

pH >2

two steps merged: $Mo_3O_4(C_2O_4)_3^{2-} \underset{-3e^-,\,-3H^+}{\overset{+3e^-,\,+3H^+}{\rightleftharpoons}} Mo_3O(OH)_3(C_2O_4)_3^{2-}$

Scheme I implies that one of the oxo groups in the Mo_3O_4 core is less basic than the other three and resists protonation in the fully reduced ion at pH values above 2. The formal potential of the resulting three-electron, three-proton reduction step would be expected to shift by 59 mV/pH unit, which is reasonably close to the slope of the line in Figure 7 at pH values above 2.

The Aquo Mo^{IV}_3 Cation. The number of water molecules coordinated to the $Mo_3O_4^{4+}$ core in aquo Mo(IV) has not been determined. On the basis of the known structures of the oxalato and edta complexes,[1,2] nine coordinated water molecules seem likely, but we will abbreviate the aquo ion as $Mo_3O_4^{4+}$. Cyclic voltammograms of $Mo_3O_4^{4+}$ in a supporting electrolyte composed of 1.0 M trifluoromethanesulfonic acid (HTFMS) and 1.0 M HCl consist of a single reduction and oxidation wave (Figure 8). The cathodic peak current increases linearly with (scan rate)$^{1/2}$ (inset in Figure 8), and the separation between the peak potentials does not depend on the scan rate. In the absence of chloride, less ideal behavior is observed with unequal anodic and cathodic peak currents.[6] In the presence of chloride, but without explicit electronic compensation to overcome uncompensated resistance in the cell, a separation of 33 mV between the peak potentials was previously interpreted as a sign of a Nernstian two-electron reduction.[6] However, a three-electron Nernstian reduction in the presence of some uncompensated cell resistance could also have produced a peak splitting in excess of the theoretical value

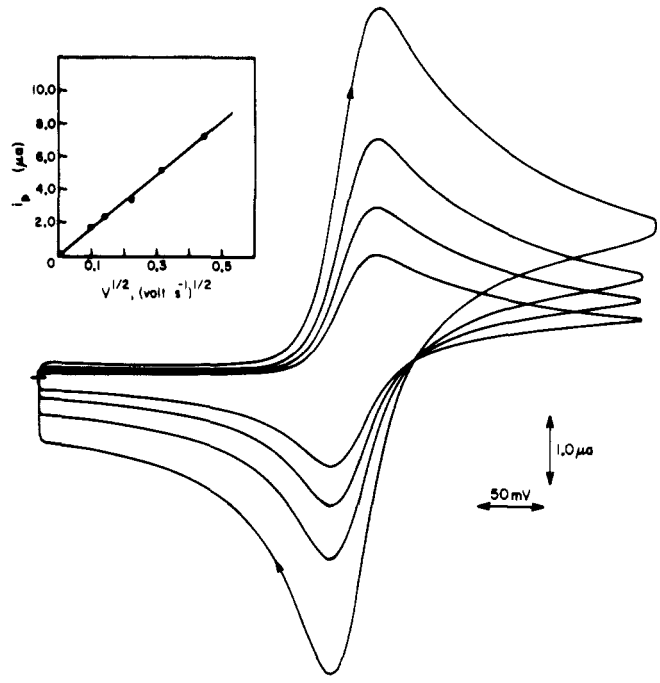

Figure 8. Cyclic voltammograms of 0.31 mM $Mo_3O_4^{4+}$ (supporting electrolyte 1 M HTFMS + 1 M HCl; initial potential −100 mV; scan rates 10, 20, 50, and 100 mV s^{-1}). Negative potentials are plotted to the left and reduction currents are plotted upward. Inset: Cathodic peak current vs. (scan rate)$^{1/2}$.

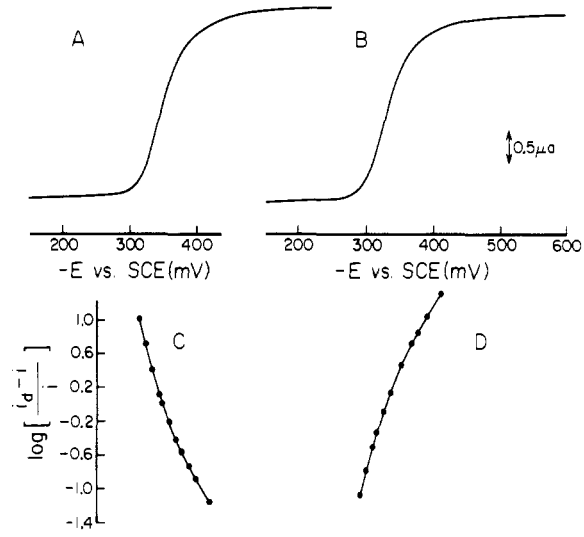

Figure 9. Normal- (A) and reverse-pulse (B) polarograms of 0.31 mM $Mo_3O_4^{4+}$ (supporting electrolyte as in Figure 8). Parts C and D are the corresponding plots of log $[(i_d - i)/i]$ vs. E (see text).

of 20 mV. One purpose of the present experiments was to check this point.

Controlled-potential electrolysis of solutions of $Mo_3O_4^{4+}$ at a mercury pool at −500 mV consumes one electron per Mo atom.[6] The resulting complex is readily reoxidized to $Mo_3O_4^{4+}$ at the electrode or by careful exposure to dioxygen.[8,9] Prolonged exposure of $Mo_3O_4^{4+}$ to dioxygen results in its eventual oxidation to Mo(VI).

Polarography. Normal- and reverse- (as well as differential-) pulse polarograms of solutions of $Mo_3O_4^{4+}$ exhibit only one apparent reduction wave in trifluoromethanesulfonic acid solutions at acid concentrations between 0.5 and 4 M. Figure 9 contains representative normal- and reverse-pulse polarograms. Logarithmic analysis of these two polarograms produced nonlinear plots (Figure 9, curves C and D). The slopes of the logarithmic plots did not depend upon the duration of

the pulses (in the presence of chloride), showing that slow electron transfer was not an important factor.[17] The slopes of the logarithmic plots are consistent with the presence of two successive reduction steps just as was true with the $Mo_3O_4(C_2O_4)_3^{2-}$ complex. However, the two formal potentials for the reduction of the $Mo_3O_4^{4+}$ appear to lie much closer to each other.

A theoretical analysis of the shapes of polarographic waves for overlapping, multistep, Nernstian electrode processes has been presented by Ruzic.[18] This treatment was applied to the case of $Mo_3O_4^{4+}$ by assuming that a two-step reduction was involved analogous to that observed with $Mo_3O_4(C_2O_4)_3^{2-}$:

$$Mo^{IV}{}_3 + 2e^- \overset{E^f_1}{\rightleftharpoons} Mo^{III}{}_2Mo^{IV} \quad (1a)$$

$$Mo^{III}{}_2Mo^{IV} + e^- \overset{E^f_2}{\rightleftharpoons} Mo^{III}{}_3 \quad (1b)$$

It is convenient to define a comproportionation equilibrium constant relating the three species depicted in eq 1.

$$2Mo^{III}{}_3 + Mo^{IV}{}_3 \rightleftharpoons 3Mo^{III}{}_2Mo^{IV} \quad (2)$$

$$K_c = \frac{[Mo^{III}{}_2Mo^{IV}]^3}{[Mo^{III}{}_3]^2[Mo^{IV}{}_3]} \quad (3)$$

K_c can also be expressed in terms of the formal potentials of the two redox steps:

$$K_c = \exp\left[\frac{n_1 n_2 F}{RT}(E^f_1 - E^f_2)\right] \quad (4)$$

where n_1 and n_2 are the number of electrons involved in the two successive steps. The ratio $(i_d - i)/i$ used in the logarithmic analysis of the polarographic wave shapes for this case can be expressed as

$$\frac{i_d - i}{i} = \frac{1}{p}\left[\frac{\frac{n_2}{n_1 + n_2}(K_c p^{n_1})^{1/(n_1+n_2)} + 1}{\frac{n_1}{n_1 + n_2}\left(\frac{K_c}{p^{n_2}}\right)^{1/(n_1+n_2)} + 1}\right] \quad (5)$$

where

$$\frac{1}{p} = \exp\left[\frac{F}{RT}[(n_1 + n_2)E - n_1E^f_1 - n_2E^f_2]\right] \quad (6)$$

and E is the potential on the polarigraphic wave corresponding to each value of i in eq 5. Plots of log $[(i_d - i)/i]$ vs. E were calculated from eq 5 for several values of $E^f_2 - E^f_1$ with n_1 = 2 and n_2 = 1 (reaction 1). The results are shown in Figure 10 along with the experimental points resulting from the corresponding plot for a normal-pulse polarogram of the reduction of $Mo_3O_4^{4+}$. Equation 5 appears to produce calculated curves with the same general morphology as the experimental curves shown in Figure 9. The experimental data fall close to the curve calculated for $E^f_2 - E^f_1 = -40$ mV. It is noteworthy that the calculated curves in Figure 10 show that clearly nonlinear logarithmic plots are to be expected for values of $E^f_2 - E^f_1$ as positive as +20 mV. If $E^f_2 - E^f_1$ is even more positive, linear plots result with slopes corresponding to the sum of n_1 and n_2.

Another useful (but not independent) method for estimating $E^f_2 - E^f_1$ is to observe the difference in potential between the points where log $[(i_d - i)/i]$ equals 1.0 and −1.0. An analogous procedure for the analysis of cyclic voltammograms was described by Meyer and Shain.[19] These potential differences (calculated from eq 5) are plotted in Figure 11 as a function of $E^f_2 - E^f_1$. When this curve was used to analyze the experimental data shown in Figure 10, a value of $E^f_2 - E^f_1$ of −(35 ± 2) mV resulted.

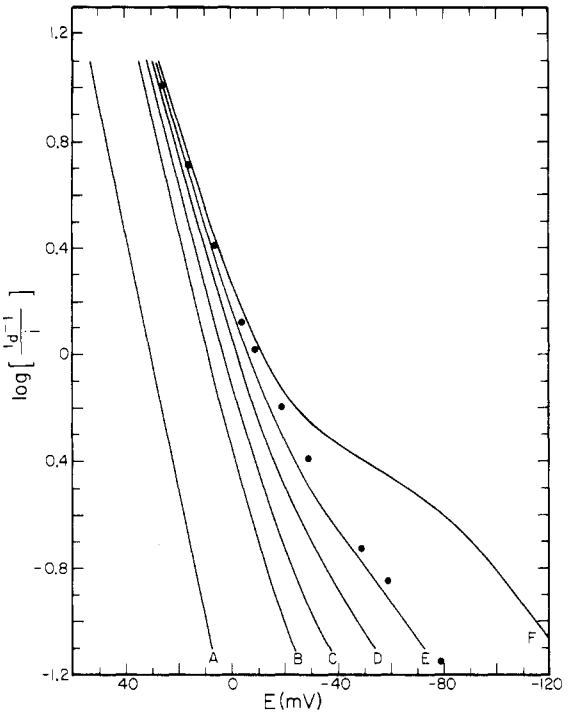

Figure 10. Plots of log $[(i_d - i)/i]$ vs. E calculated from eq 5 for different values of $E^f_2 - E^f_1$. The experimental points (●) were taken from Figure 9C. Values of $E^f_2 - E^f_1$ were (A) +90, (B) +20, (C) 0, (D) −20, (E) −40, and (F) −90 mV.

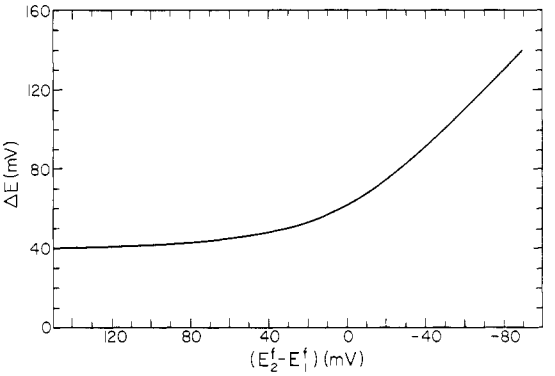

Figure 11. Separation in the potentials where log $[(i_d - i)/i]$ equals +1.0 and −1.0 as a function of $E^f_2 - E^f_1$ (evaluated from the curves in Figure 10).

Cyclic Voltammetry. The cyclic voltammetric response to be expected from a two-step Nernstian electrode reaction that proceeds according to reaction 1 can be calculated by means of a digital simulation procedure described recently by Sokol et al.[20] Application of this procedure to the present case gave the best agreement between the experimental and calculated voltammograms with $E^f_2 - E^f_1$ set equal to −36 mV (and n_1 = 2 and n_2 = 1). A comparison is shown in Figure 12A. The agreement is excellent for the cathodic portion of the wave, but deviations appear in the anodic portion. The same behavior was also observed by Sokol et al.,[20] who attributed them to difficulties in making adequate corrections for the background

(17) Fonds, A.; Brinkman, A.; Los, J. *J. Electroanal. Chem. Interfacial Electrochem.* **1967**, *14*, 43.
(18) Ruzic, I. *J. Electroanal. Chem. Interfacial Electrochem.* **1970**, *25*, 144.
(19) Meyers, R.; Shain, I. *Anal. Chem.* **1969**, *41*, 980.
(20) Sokol, W.; Evans, D.; Niki, K.; Yagi, T. *J. Electroanal. Chem. Interfacial Electrochem.* **1980**, *108*, 107.

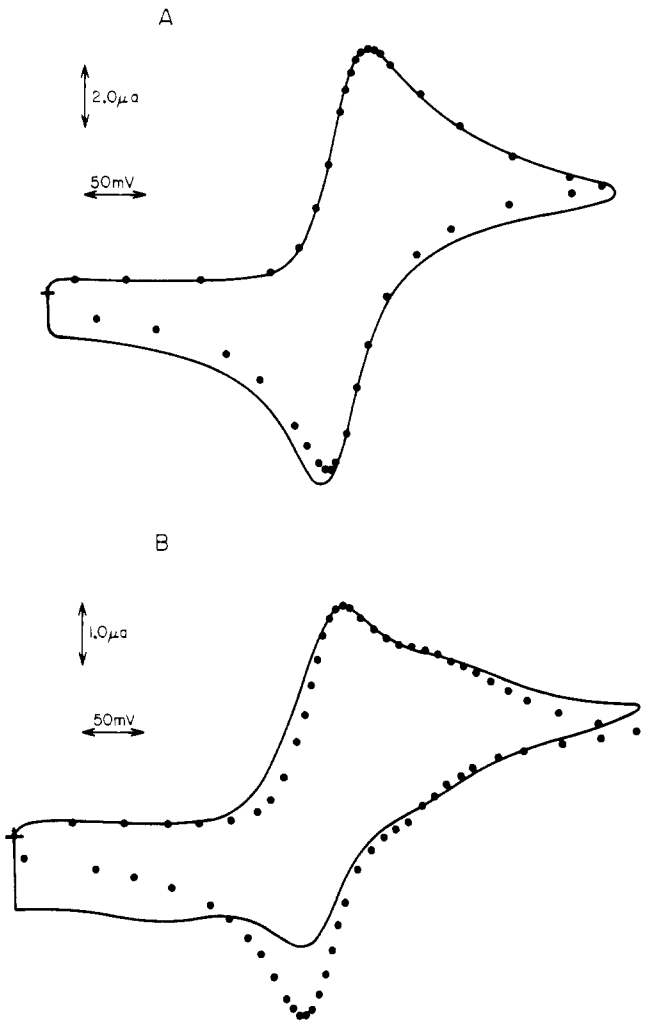

Figure 12. Experimental (solid line) and simulated (points) cyclic voltammograms for $Mo_3O_4^{4+}$ (initial potential −100 mV): (A) supporting electrolyte 1 M HTFMS + 1 M HCl, scan rate 200 mV s^{-1}; (B) supporting electrolyte 2 M HPTS, scan rate 50 mV s^{-1}.

current during the second half of a cyclic voltammogram. The good agreement we observed for the cathodic portion of the wave adds further support to our supposition that eq 1 represents a realistic picture of the pathways involved in the electroreduction of $Mo_3O_4^{4+}$.

Acid Dependence of the Half-Wave Potential for $Mo_3O_4^{4+}$ Reduction. The dependence of $E_{1/2}$ for the composite normal-pulse polarographic wave for the reduction of $Mo_3O_4^{4+}$ on the concentration of protons is shown in Figure 13. The Hammet acidities of each solution, H_o, were evaluated from spectral measurements with *o*-nitroaniline.[21] The nonlinearity of the plot is to be expected if the two steps identified in reaction 1 have different acid dependences. At the lower acidities ($H_o \leq 0.1$) a limiting slope of ca. 60 mV/H_o unit results while at higher acidities the slope increases to ca. 90 mV/H_o unit. These data show that protons are consumed in the reduction reaction throughout the range of acidities tested. To dissect the acid dependence into its component parts, Figure 11 was used to obtain values of $E^f_2 - E^f_1$ from the logarithmic analysis of polarograms recorded in solutions of varying acidity. (The limits on the range of acidities tested were set on the high side by the desire to maintain constant ionic strength and on the low side by changes in the structure of the $Mo_3O_4^{4+}$ core at acidities below ca. 0.1 M.[7]) A plot of the resulting values of $E^f_2 - E^f_1$ vs. H_o is shown in Figure 14. The data fall on

(21) Paul, M.; Long, F. *Chem. Rev.* **1957**, *57*, 1.

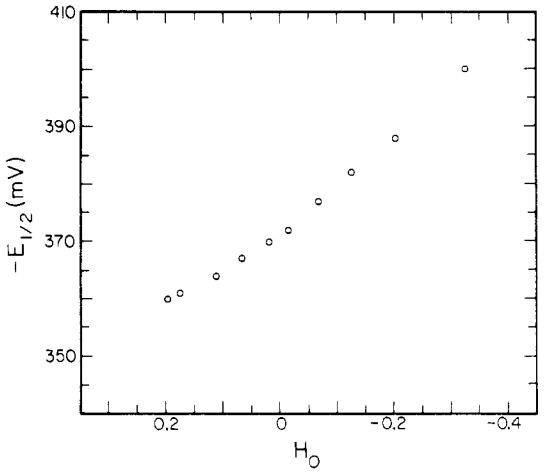

Figure 13. Polarographic half-wave potential vs. Hammett acidity function, H_o, for reduction of $Mo_3O_4^{4+}$. Supporting electrolyte was 0.1 M HCl + HTFMS + LiTFMS adjusted to maintain an ionic strength of 2.0 M.

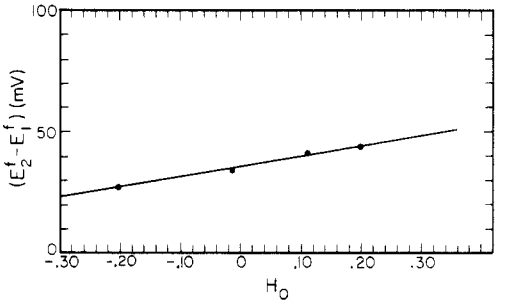

Figure 14. Values of $E^f_2 - E^f_1$ evaluated from Figure 11 plotted vs. H_o.

a straight line of slope 43 ± 5 mV/H_o unit. A number of possible acid dependences of the two reduction steps in reaction 1 were considered to account for the slope of the line in Figure 14. The closest correspondence results if the first, two-electron, step consumes three protons and the second, one-electron, step consumes one additional proton as depicted in Scheme II. The slope of a plot of $E^f_2 - E^f_1$ vs. H_o would be predicted to be 30 mV/H_o unit on the basis of Scheme II. The observed slope (43 ± 5 mV) does not seem unreasonable considering the possible sources of error in the many measurements that were required for the preparation of Figure 14.

Scheme II

$$\text{first step: } Mo_3O_4^{4+} \underset{-2e^-,\,-3H^+}{\overset{E^f_1\ +2e^-,\,+3H^+}{\rightleftharpoons}} Mo_3O(OH)_3^{5+}$$

$$\text{second step: } Mo_3O(OH)_3^{5+} \underset{-e^-,\,-H^+}{\overset{E^f_2\ +e^-,\,+H^+}{\rightleftharpoons}} Mo_3(OH)_4^{5+}$$

Absorption Spectra. UV–visible absorption spectra of solutions containing only Mo^{IV}_3 or only Mo^{III}_3 in 0.5–4 M HTFMS agreed with those reported previously.[8,9] However, similar solutions containing mixtures of these two ions and, therefore, $Mo^{III}_2Mo^{IV}$ ion as well, produced somewhat different spectra. To see whether this difference was a property of the acidic electrolyte utilized in the previous work (*p*-toluenesulfonic acid, HPTS), we also recorded spectra of 2:1 mixtures of Mo^{III}_3 and Mo^{IV}_3 in this acid. The resulting spectra were identical with those reported previously.[8,9]

***p*-Toluenesulfonic Acid Media.** The dependence of the absorption spectra on the nature of the acid led us to examine the electrochemical behavior of Mo^{IV}_3 in HPTS. A cyclic

Table I. Evaluation of Formal Potentials and the Comproportionation Equilibrium Constant

$[H^+]$,[a] M	$-E^f_1$,[b] mV	$-E^f_2$,[c] mV	$-(E^f_2 - E^f_1)$, mV	K_c[d]
4.10	305	351	46.0	36[e]
2.00	345.5	389	43.5	30
1.52	353.5	395	41.5	25
1.12	364	398	34.0	14
0.64	382.5	409.5	27.0	8

[a] Except for $[H^+] = 4.1$ M, all solutions were prepared from trifluoromethanesulfonic acid, 0.1 M HCl, and sufficient lithium trifluoromethanesulfonate to maintain an ionic strength of 2.0 M. [b] Formal potential of step 1 in Scheme II. [c] Formal potential of step 2 in Scheme II. [d] Equilibrium constant for reaction 2. [e] Solution contained only 4.1 M HTFMS.

voltammogram for Mo^{IV}_3 in 2 M HPTS is shown as the solid line in Figure 12B. The presence of two reduction steps is evident, indicating that the separation between the formal potentials of the two steps is larger in HPTS than in HTFMS supporting electrolytes. Normal-pulse polarograms were recorded in 2 M HPTS, and their shapes were analyzed by means of the curve in Figure 11 to estimate a 68-mV separation between the formal potentials of the two reduction steps. In 4 M HPTS the apparent difference in the two formal potentials increases to ca. 106 mV so that the two stages of the reduction are even more clearly distinguishable. Thus, in HPTS the reduction of Mo^{IV}_3 appears more similar to that of $Mo_3O_4(C_2O_4)_3^{2-}$ than it does in HTFMS supporting electrolytes.

Estimation of Formal Potentials and Comproportionation Constant. The formal potentials of the half-reactions in Scheme II and the equilibrium constant for reaction 2 were estimated at several concentrations of HTFMS from an analysis of the shapes of normal-pulse polarograms by means of the curve in Figure 11. The resulting values of $E^f_2 - E^f_1$ were substituted in eq 4 to obtain the values of K_c listed in Table I. The variation of $E^f_2 - E^f_1$ and, therefore, of K_c with acidity is much smaller than that reported by Richens and Sykes in HPTS electrolytes.[9] As a result, and in contrast with HPTS,[9] reaction 2 cannot be forced to proceed completely to the right and the two reduction waves of Mo^{IV}_3 cannot be completely separated by increasing the concentration of HTFMS. The values of E^f_1 and E^f_2 in Table I are similar in magnitude to some of the "reduction potentials" reported by Richens and Sykes, but we believe they refer to distinctly different half-reactions for reasons to be discussed.

The Aquo Mo^{III}_3 Cation. Cyclic voltammograms for a solution of Mo^{III}_3 produced by controlled-potential reduction of $Mo_3O_4^{4+}$ are shown in Figure 15. Two anodic peaks are clearly evident. This contrasts with the anodic response shown in Figure 8 during the second half of cyclic voltammograms recorded with solutions of $Mo_3O_4^{4+}$ where only a single anodic peak appears. The implication is that a portion of the Mo^{III}_3 formed initially from the reduction of Mo^{IV}_3 undergoes some structural rearrangement on the time scale of controlled-potential electrolysis (up to several hours) to produce a form that is reoxidized at a more positive potential than the unrearranged Mo^{III}_3. The rearrangement would have to proceed too slowly to be detected by cyclic voltammetry at scan rates as low as 10 mV s^{-1} (Figure 8) or by reverse-pulse polarography with a drop time of 1 s (Figure 9). To test this supposition, solutions of Mo^{III}_3 were prepared as rapidly as possible by pouring solutions of Mo^{IV}_3 through a column of zinc metal. (The Zn^{2+} ion introduced into the solution was reduced at potentials outside the range of interest and therefore did not interfere.) The resulting solutions were examined periodically by the sensitive method of differential-pulse polarography to detect if one or two waves were present in the responses. The results,

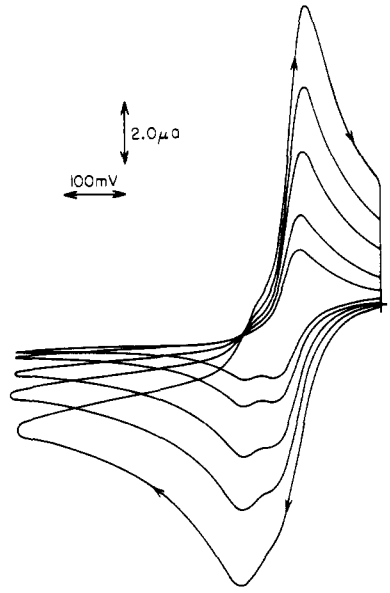

Figure 15. Cyclic voltammograms of Mo^{III}_3 produced by controlled-potential reduction of Mo^{IV}_3 (supporting electrolyte 2 M HTFMS; initial potential −500 mV; scan rates 10, 20, 50, 100, and 200 mV s^{-1}). Negative potentials are plotted to the left and reduction currents are plotted upward.

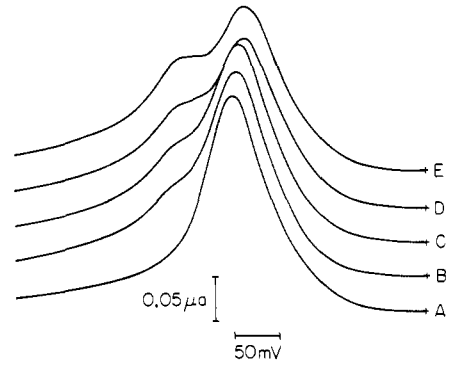

Figure 16. Differential-pulse polarograms of a solution of Mo^{III}_3 at various times after its preparation by rapid reduction with zinc metal. The age of the solution was (A) 20 min and (B) 8, (C) 12, (D) 22, and (E) 36 h (initial potential −550 mV). Between recordings the solution was stirred with argon over a mercury pool maintained at −550 mV.

shown in Figure 16, demonstrate that the second wave begins to appear after ca. 2 h and reaches its final magnitude after ca. 30 h under the experimental conditions employed. This time dependence of the relative magnitudes of the two waves in solutions containing only Mo^{III}_3 shows clearly that the species initially formed reacts to produce a more difficultly oxidized form of the same net oxidation state. Since cyclic voltammograms of the solutions showed only a single reduction wave under all conditions, the two forms of Mo^{III}_3 are apparently oxidized to the single, stable form of Mo^{IV}_3. This interpretation does not correspond to that proposed by Richens and Sykes, who also reported two oxidation waves for Mo^{III}_3 under some conditions.[8,9] The reasons that we prefer our interpretation are given in the Discussion.

ESR Spectra of Mo^{III}_3. Solutions of Mo^{III}_3 produced ESR spectra such as that shown in Figure 4B. The similarity between the spectra for the aquo and oxalato complexes suggests similar structures for the two ions. Both spectra were eliminated by electrochemical reoxidation of the reduced ions. When a solution of $Mo_3O_4^{4+}$ in 2 M trifluoromethanesulfonic acid was electrolytically reduced by one-third electron per molybdenum atom, an ESR spectrum identical with that in

Figure 4B was obtained but its intensity was only about 10% of that resulting when the electrolysis was carried to completion. The failure of the spectrum's intensity to follow linearly the extent of reduction points to a rapid equilibrium among the various species present with appreciable equilibrium concentrations of all three of the species depicted in Scheme II.

Discussion

Comparison of $Mo_3O_4(C_2O_4)_3^{2-}$ and $Mo_3O_4^{4+}$. The mechanism of the electroreduction of $Mo_3O_4(C_2O_4)_3^{2-}$ is reasonably transparent at acidities where the two reduction steps are well separated. The overall reduction proceeds as indicated in Scheme I. The difference in the pH dependences of the first and second steps accounts for the merging of the two waves at pH values above 2.

In solutions of *p*-toluenesulfonic acid (HPTS) the electrochemical behavior of the aquo Mo^{IV}_3 cation $Mo_3O_4^{4+}$ parallels that of the oxalato complex. Adjustment of the formal potentials of the two reduction steps by control of the acid concentration allows large equilibrium concentrations of the partially reduced ion $Mo^{III}_2Mo^{IV}$ to be generated. By contrast, in trifluoromethanesulfonic acid (HTFMS) solutions the smaller separation of the formal potentials for the two reduction steps of $Mo_3O_4^{4+}$ and their lesser pH dependence leads to much greater disproportionation of the partially reduced ion under all experimentally accessible conditions. This prevented us from using spectral data to evaluate the equilibrium compositions of solutions of $Mo^{III}_2Mo^{IV}$ in HTFMS at any of the concentrations where Richens and Sykes were able to do so in HPTS.[9] The acidities of equally concentrated solutions of HPTS and HTFMS do not differ greatly (as judged from the ratio of protonated to unprotonated *o*-nitroaniline in the two solutions) so that the difference in the electrochemical responses of $Mo_3O_4^{4+}$ in the two acids probably arises from differences in specific ionic interactions between the molybdenum cations and the PTS^- or $TFMS^-$ anions.

Mo^{III}_3 Aquo Ion. The pair of anodic peaks in the voltammogram for an aged solution of Mo^{III}_3 (Figure 15) and the single oxidation peak obtained during the oxidizing half of cyclic voltammograms for solutions of Mo^{IV}_3 (Figure 8) clearly point to the occurrence of a chemical reaction subsequent to the electroreduction of Mo^{IV}_3. Similar behavior was reported by Richens and Sykes,[9] who attributed the double peaks to the existence of two slowly interconverting forms of $Mo^{III}_2Mo^{IV}$, only one of which could be further reduced to Mo^{III}_3. The implication was that Mo^{IV}_3 was reduced only to the irreducible form of $Mo^{III}_2Mo^{IV}$ on the time scale of cyclic voltammetry so that only a single reoxidation wave appeared. The longer times involved in controlled-potential electrolyses were presumed adequate for some rearrangement of the initially formed $Mo^{III}_2Mo^{IV}$ species followed by its further reduction to Mo^{III}_3. The two waves observed in voltammograms for the oxidation of Mo^{III}_3 were then presumably ascribed (ref 9 is not explicit on this point) to the formation of the second form of $Mo^{III}_2Mo^{IV}$ followed by its further oxidation to Mo^{IV}_3 without a slow structural rearrangement being required.

This interpretation suffers from the fact that it predicts a voltammetric peak current for the reduction of Mo^{IV}_3 that corresponds to two rather than three electrons. This is not observed. A further predicted consequence would be a normal-pulse-polarographic limiting current for the reduction of Mo^{IV}_3 that is two-thirds as large as that for the oxidation of an equilibrated solution of Mo^{III}_3. In fact, the limiting currents for these two solutions are virtually identical. Thus, the two forms of $Mo^{III}_2Mo^{IV}$ proposed by Richens and Sykes[9] are not compatible with the observed electrochemical responses.

The most compelling evidence that the chemical transformation involved occurs at the level of Mo^{III}_3 is contained in

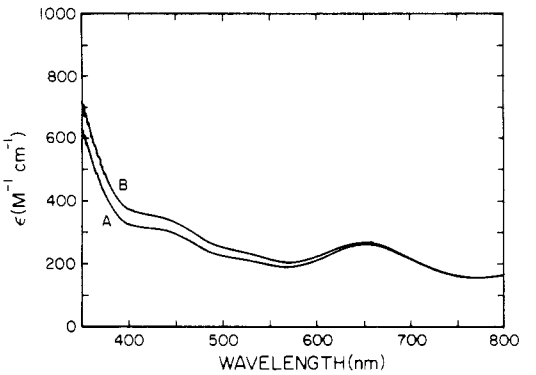

Figure 17. Spectra of Mo^{III}_3 (A) immediately after preparation and (B) after 48 h.

Figure 16: The second peak in the differential-pulse polarogram of solutions of Mo^{IV}_3 that have been rapidly reduced to Mo^{III}_3 develops as the fully reduced solution stands. Thus, it appears that two electrochemically distinguishable forms of Mo^{III}_3 are generated in these solutions. The spectrum of freshly reduced solutions of Mo^{III}_3 that exhibit just one anodic peak differs only slightly from that of an aged solution that exhibits two peaks (Figure 17), and both forms of Mo^{III}_3 are readily oxidized to the same Mo^{IV}_3 species. The structural differences between the two forms of Mo^{III}_3 (including the possibility that one form may contain more than three Mo atoms) remain to be elucidated. However, the existence of two electrochemically distinct forms of Mo^{III}_3 means that there are two formal potentials connecting the Mo^{III}_3 and $Mo^{III}_2Mo^{IV}$ oxidation states to be considered. The values given in Table I were obtained under conditions where only freshly formed Mo^{III}_3 was present so that they represent the formal potential relating $Mo^{III}_2Mo^{IV}$ and the initial form of Mo^{III}_3. Both the magnitudes and the assignments of the formal potentials given in ref 9 require some revision in the light of these results.

Concluding Remarks

The trinuclear Mo^{IV}_3 ion is reduced in a two-electron step followed by a one-electron step at potentials that are very close together. The reasons for this reductive pattern are presumably related to structural changes that accompany the reductions. A relevant molecular orbital calculation of Cotton[22] and more recent calculations[23] suggest that the addition of electrons to the $Mo_3O_4^{4+}$ core results in increased electron density on the bridging and capping oxo groups. This is consistent with the coupled electron–proton reduction steps outlined in Scheme II in which the formation of hydroxo groups is indicated in the reduced products.

It is interesting to note that molybdenum in oxidation state III is now known to form at least three simple aquo ions: monomeric $Mo(OH_2)_6^{3+}$,[24] dimeric $Mo_2(OH)_2^{4+}$,[7] and the trimeric ion whose core composition is believed to be $Mo_3(OH)_4^{5+}$. In addition, the results presented here indicate that there are two electrochemically distinct forms of the trimeric ion. Only the trimeric ion is electrooxidizable to the trimeric molybdenum(IV) ion, $Mo_3O_4^{4+}$. $Mo(OH_2)_6^{3+}$ is electrooxidized with difficulty[6] and yields the molybdenum(V) dimer $Mo_2O_4^{4+}$. $Mo_2(OH)_2^{4+}$ is electrooxidized more readily to the same product.[6] $Mo(OH_2)_6^{3+}$ apparently undergoes slow spontaneous condensation possibly to $Mo_2(OH)_2^{4+}$,[24] but the relative thermodynamic stabilities of the dimeric and trimeric

(22) Cotton, F. *Inorg. Chem.* **1964**, *3*, 1217.
(23) Bursten, B.; Cotton, F.; Hall, M.; Najjar, R. *Inorg. Chem.* **1982**, *21*, 302.
(24) Bowen, R.; Taube, H. *J. Am. Chem. Soc.* **1971**, *93*, 3287.

forms of aqua Mo(III) remain to be established.

Acknowledgment. This work was supported by the National Science Foundation. Helpful discussions with Dr. Daniel Polcyn and Professor Dennis Evans are gratefully acknowledged.

Registry No. $Cs_2Mo_3O_4(C_2O_4)_3(H_2O)_3$, 85165-04-4; $Mo_3O_4(C_2O_4)_3^{2-}$, 85165-05-5; $Mo_3O_4^{4+}$, 74353-85-8; $Mo_3(OH)_4(C_2O_4)_3^{-}$, 85096-90-8; $Mo_3(OH)_4(C_2O_4)_3$, 85096-91-9; HPTS, 104-15-4; HTFMS, 1493-13-6.

Contribution from Rocketdyne,
A Division of Rockwell International Corporation, Canoga Park, California 91304

Synthesis of *N,N*-Difluoro-*O*-perhaloalkylhydroxylamines. 2. Lewis Acid Catalyzed Addition of NF_3O to Olefins

RICHARD D. WILSON, WALTER MAYA,[1a] DONALD PILIPOVICH,[1b] and KARL O. CHRISTE*

Received June 15, 1982

N,N-Difluoro-*O*-perhaloalkylhydroxylamines, R_fONF_2, were successfully prepared by the Lewis acid catalyzed addition of NF_3O to olefins. The new compounds $XC_2F_4ONF_2$ (X = F, Cl, Br) were obtained and characterized. The unexpected direction of the NF_3O addition, resulting exclusively in the anti-Markownikoff-type isomer $XCF_2CF_2ONF_2$, was elucidated by model reactions involving the stepwise addition of BF_3 and NF_3O to $CF_2{=}C{=}CF_2$. It is shown that all reactions can be rationalized in terms of an R_fBF_2 intermediate produced by the normal polar addition of BF_3 to the olefin. In the case of $CF_2{=}C{=}CF_2$, the new vinyldifluoroborane $CF_2{=}C(BF_2)CF_3$ was isolated and characterized. Attempts to isolate $-ONF_2$-substituted vinyl compounds by reaction of NF_3O with vinyldifluoroboranes led to difluoramino ketones formed via a keto–enol-type tautomerism.

Introduction

Following the discosvery of NF_3O in 1961 by Rocketdyne[2] and Allied Chemical,[3] studies were carried out in these two laboratories to add NF_3O to olefinic double bonds. Except for an incomplete description of some of the Rocketdyne results in a patent[4] and a one-sentence statement in a paper on NF_3O by the Allied group,[3] these data have not been published, partially due to their incompleteness and the lack of a plausible mechanism to explain the observed direction of the NF_3O addition. The previous Rocketdyne studies have now been complemented and are summarized in this paper.

Experimental Section

Caution! The addition reactions of NF_3O to olefins, particularly hydrogen-containing compounds, can proceed explosively. Appropriate safety precautions must be taken when these reactions are carried out.

Materials and Apparatus. The apparatus, handling techniques, and instrumental conditions used in this study have been described in part 1 of this series.[5] Literature methods were used for the syntheses of NF_3O,[6] $CF_2{=}C{=}CF_2$,[7] and $CF_2{=}CFBF_2$.[8] Monomeric $CF_2{=}CF_2$ was prepared by vacuum pyrolysis of poly(tetrafluoroethylene); C_2F_3Cl and BF_3 (The Matheson Co.) and C_2F_3Br (Ozark Mahoning Co.) were purified by fractional condensation prior to their use.

Syntheses of $XCF_2CF_2ONF_2$. Most reactions of NF_3O in the presence of BF_3 with C_2F_4, C_2F_3Cl, or C_2F_3Br were carried out according to the following general procedure. Equimolar amounts (3 mmol each) of C_2F_3X (X = F, Cl, Br) and BF_3 were condensed at −196 °C into the tip of a 250-mL Pyrex reactor. The mixture was warmed for 2 h to −78 °C and then recooled to −196 °C. An equimolar amount of NF_3O (3 mmol) was condensed at −196 °C above the C_2F_3X–BF_3 mixture. The reactor was allowed to warm slowly to −78 °C and was kept at this temperature for several hours before being allowed to warm to ambient temperature. The volatile materials were separated by fractional condensation through a series of traps at −78 °C, at −95 °C (for C_2F_3Br reaction), or −112 °C (for C_2F_3Cl reaction), or −142 °C (for C_2F_4 reaction), and at −196 °C. The −78 °C trap contained small amounts of unidentified material. The −196 °C trap contained mainly unreacted BF_3, C_2F_3X, C_2F_5X, and sometimes small amounts of NF_3O. The −95, −112, or 142 °C trap contained the desired $XC_2F_4ONF_2$ product. The reactor generally contained some white solid residue, which according to its spectra consisted of $NOBF_4$. The yields of $C_2F_5ONF_2$, $CF_2ClCF_2ONF_2$, and $CF_2BrCF_2ONF_2$ were about 60, 18, and 10%, respectively. Whereas $C_2F_5ONF_2$ could be obtained in high purity by the above described simple fractionation, $ClC_2F_4ONF_2$ and $BrC_2F_4ONF_2$ contained about 10% of an unidentified halocarbon impurity whose removal required either repeated careful fractionations or gas chromatographic techniques.

$CF_3{}^{A}CF_2{}^{B}ONF_2{}^{C}$: bp −24.9 °C; mp −146.5 °C; mol wt found 185; mol wt calcd 187; $\log [P\ (\text{mm})] = 8.0222 - 1271/[T\ (\text{K})]$; ΔH_{vap} = 5.8 kcal/mol; Trouton constant 23.5; mass spectrum (70 eV) [*m/e* (intensity) ion], 119 (69) $C_2F_5^+$, 100 (3.4) $C_2F_4^+$, 69 (100) CF_3^+, 66 (2.1) CF_2O^+, 52 (29) NF_2^+, 50 (10) CF_2^+, 47 (7.1) CFO^+, 33 (7.7) NF^+, 31 (12) CF^+, 30 (24) NO^+, 19 (1.1) F^+, 16 (0.3) O^+; ^{19}F NMR (positive shifts are low field from $CFCl_3$) neat ϕ_A (tr tr = sept) −89.0, Φ_B (quart tr) −95.9, ϕ_C (br tr) 124.9, $CFCl_3$ solvent ϕ_A −85.9, ϕ_B −93.0, ϕ_{C3} 128.1 (J_{AB} = 2.02, J_{AC} = 1.01, J_{BC} = 3.0, J_{NC} = 110 Hz); IR 2640 (vw), 2600 (vvw), 2478 (vw), 2408 (vw), 2350 (vvw), 2317 sh, 2235 (vw), 2090 (vvw), 2050 (vw), 1984 (vw), 1931 (vw), 1867 (vw), 1815 sh, 1791 (vw), 1775 sh, 1679 (vw), 1594 (vw), 1510 (vw), 1471 (vvw), 1401 (mw), 1300 sh, 1247 (vs), 1206 (vs), 1114 (vw), 1028 (vs), 903 (s), 850 (vs), 741 (m, PQR), 730 sh, 660 (w), 621 (vw), 569 (vw),531 (mw), 474 (vvw), 462 (vvw), 444 (vvw) cm^{-1}; Raman (liquid −90 °C) 1402 (0.7), 1240 (0.1), 1205 (0.1), 1111 (1.2) p, 1025 (6.6) p, 903 (0.7) dp, 849 (2.4) p, 835 (1.2) p, 741 (10) p, 659 (2.8) p, 619 (0.7) dp, 570 (3.1) p, 559 (0.2) dp, 529 (0.2) dp, 466 (0.2) dp, 442 (0.1) dp, 358 (1.7) p, 342 (1.9) dp, 303 (6.2) p, 244 (4.1) p, 121 (0.6) dp cm^{-1}. Anal. Calcd for C_2F_7NO: N, 7.48. Found: N, 7.21 (N_2 by evolution by Na reduction).

$ClCF_2{}^{A}CF_2{}^{B}ONF_2{}^{C}$: bp 13.8 °C; mol wt found 204.6; mol wt calcd 203.5; $\log [P\ (\text{mm})] = 7.6002 - 1355/[T\ (\text{K})]$; Δ_{vap} = 6.2 kcal/mol; Trouton constant 21.6; mass spectrum (70 eV) [*m/e* (intensity) ion] 137 (16.2) $C_2F_4{}^{37}Cl^+$, 135 (52.3) $C_2F_4{}^{35}Cl^+$, 119 (20.7) $C_2F_5^+$, 118 (0.6) $C_2F_3{}^{37}Cl^+$, 116 (1.9) $C_2F_3{}^{35}Cl^+$, 100 (9) $C_2F_4^+$, 87 (32) $CF_2{}^{37}Cl^+$,

(1) Present addresses: (a) Department of Chemistry, California State University, Pomona, CA 91768; (b) MVT, Microcomputer Systems Inc., Westlake Village, CA 91361.
(2) Maya, W. U. S. Patent 3 320 147, 1967.
(3) Fox, W. B.; MacKenzie, J. S.; Vaanderkooi, N.; Sukornick, B.; Wamser, C. A.; Holmes, J. R.; Eibeck, R. E.; Stewart, B. B. *J. Am. Chem. Soc.* **1966**, *88*, 2604.
(4) Pilipovich, D. U.S. Patent 3 440 251, 1969.
(5) Maya, W.; Pilipovich, D.; Warner, M. G.; Wilson, R. D.; Christe, K. O. *Inorg. Chem.* **1983**, *22*, 810.
(6) Maya, W. *Inorg. Chem.* **1964**, *3*, 1063.
(7) Jacobs, T. L.; Bauer, R. S. *J. Am. Chem. Soc.* **1956**, *78*, 4815.
(8) Stafford, S. L.; Stone, F. G. A. *J. Am. Chem. Soc.* **1960**, *82*, 6238.

0020-1669/83/1322-1355$01.50/0